Molecular Crystals and Liquid Crystals Science and Technology. Section A. Molecular Crystals and Liquid Crystals

Publication details, including instructions for authors and subscription information:
http://www.tandfonline.com/loi/gmcl19

Optical Characterization of Electroconvection in Nematics

Heidrun Amm [a], Maren Grigutsch [a] & Ralf Stannarius [a]

[a] Universität Leipzig, Fakultät für Physik und Geowissenschaften, Linnéstr. 5, Leipzig, D-04103, Germany

Version of record first published: 24 Sep 2006

To cite this article: Heidrun Amm, Maren Grigutsch & Ralf Stannarius (1998): Optical Characterization of Electroconvection in Nematics, Molecular Crystals and Liquid Crystals Science and Technology. Section A. Molecular Crystals and Liquid Crystals, 320:1, 11-27

To link to this article: http://dx.doi.org/10.1080/10587259808024380

Mol. Cryst. Liq. Cryst., Vol. 320, pp. 11–27
Reprints available directly from the publisher
Photocopying permitted by license only

Optical Characterization of Electroconvection in Nematics

HEIDRUN AMM, MAREN GRIGUTSCH, AND RALF STANNARIUS
Universität Leipzig, Fakultät für Physik und Geowissenschaften,
Linnéstr. 5, Leipzig, D-04103, Germany

We describe non-standard techniques for optical studies of electroconvection structures in nematics. The time-resolved textures in the high frequency oscillatory regime are analyzed and compared with results of optical simulations. Conclusions on the relation between director pattern and optical texture are drawn. Using an additional phase plate in the optical set-up, we monitor director twist deformations in the convection structures which are usually neglected. We demonstrate their role in the evolution of the chevron texture.

Keywords: liquid crystals; electroconvection; optical characterization

INTRODUCTION

Electrohydrodynamic convection (EHC) in nematics is a fundamental standard system in dissipative pattern formation. The undiminished interest in the study of EHC originates basically from its excellent model character for other pattern forming systems, an easy control of the system parameters, the variety of patterns which are formed and their straightforward experimental observability. The fundamental properties of EHC structures in nematics are well known (for a recent review see, e.g.[1]), their first theoretical explanation has been given by Carr and Helfrich[2] and the theoretical description has been consequently developed since (e.g.[3–6]). Optical investigations play the dominating role in the characterization of EHC structures in liquid crystals. In the standard set-up, the optical

transmission texture in nematic cells is analyzed by means of polarizing microscopy. The texture observed results from the distortion of the wave front of the parallel incident light in the spatially inhomogeneous director field and the deflection of the propagation direction of light rays. Wavelengths and orientations of the convection rolls can be easily extracted, additional informations on the director tilt profile can be obtained from comparison of experiment and optical simulations (e.g.[7 12]).

We describe the use of some non-standard optical techniques which provide information on the director structure in the convection patterns. We consider samples in planar geometry. Patterns in the low frequency conduction regime have been extensively studied by many researchers in the past, we refer to the review in Ref.[1] and refs. therein. In this paper, we concentrate our studies on patterns in the high frequency dielectric regime, above the cut-off frequency. We record time resolved transmission textures and demonstrate their relation to the director oscillations, and in a second experiment we describe the role of the director twist during the formation of the chevron texture.

EXPERIMENT

The experiments have been performed with a mixture of four disubstituted phenyl-benzoates *(Mischung 5)*

n(O)-Om: $C_nH_{2n+1} - (O) -$ 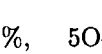 $- COO -$  $- O - C_mH_{2m+1}$

1O-O6: 22.0%, 5O-O8: 30.3%, 6O-O7: 13.3%, 6 -O4: 34.4%.

which is nematic at room temperature. Its clearing point is 70.5°C, and the nematic phase can be supercooled below 0°C.

At 30°C, the elastic constants of *Mischung 5* are $K_{11} = 14.9$ pN, $K_{22} = 6.10$ pN, and K_{33}=13.76 pN, the rotational viscosity is γ_1=0.36 Pa s, conductivities are $\sigma_{\|} = 1.3 \cdot 10^{-8}$ S/m, $\sigma_{\perp} = 1.0 \cdot 10^{-8}$ S/m, dielectric constants are $\epsilon_{\|}$=6.24, $\epsilon_{\perp}$=6.67[13], $\epsilon_{\|} - \epsilon_{\perp}$ is negative.

We have used commercial glass cells (LINKAM) with transparent ITO electrodes and rubbed polyimide coating (planar anchoring), the cell thickness was 50.5μm. The homogeneous ground state of the director field is along the rubbing direction $\vec{n}_0$. Fig. 1 shows the onset threshold of convection structures in the investigated system when the sample is driven with square wave AC electric fields.

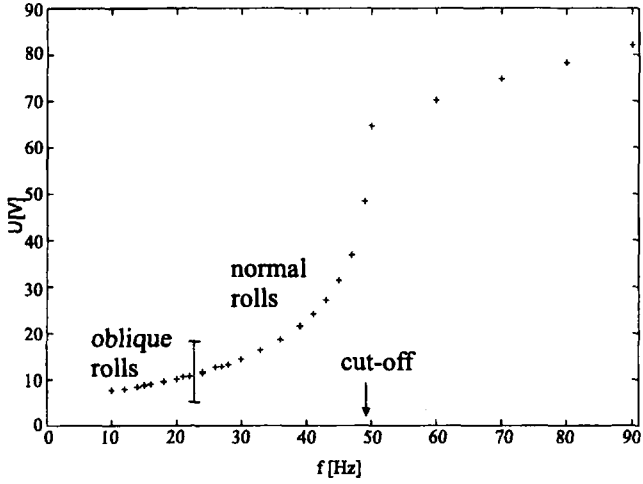

FIGURE 1 Threshold diagram of electroconvection patterns in a 50.5μm planar cell at 30°C, the cut-off is at 49Hz. Only the threshold U_C of the first instability is marked.

For the observation of convection rolls, the standard optical setup (Fig. 2a) was used, while for the visualization of director twist, we have inserted an additional $\lambda/4$ phase plate between cell and analyzer (Fig. 2b).

The polarizing microscope used in the experiments was a JENAPOL-d. Stationary video images were taken with a HAHAMATSU CCD camera and C2400 camera controller. Time resolved images were recorded with a fast 512 pixel line scan camera (DALSA Cl-C3-0512M) and digitized with an OCULUS OD 500 frame grabber. The scan rate was 1ms/line. The spatial resolution was $\approx 0.7\mu$m per camera pixel. Images were digitized

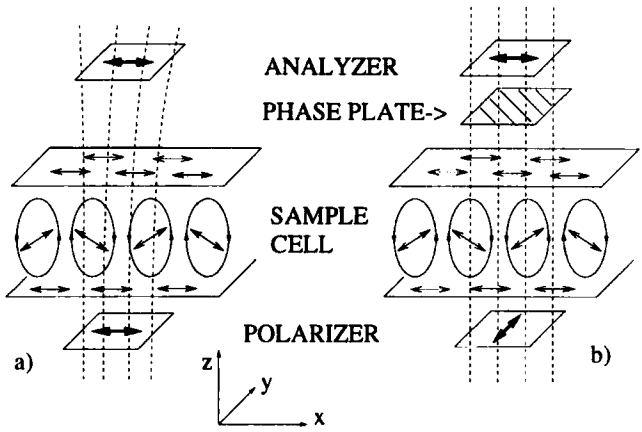

FIGURE 2 a) Standard optical setup for the observation of the director tilt structure, polarizers $\|\vec{n}_0$. Refraction of transmitted light is sketched. b) Director twist is monitored by a $\lambda/4$ plate in 45° orientation, polarizer $\perp \vec{n}_0$.

and analyzed with image processing software (IDL). Temperature was controlled with a LINKAM hot stage.

RESULTS

In the threshold diagram of Fig. 1 (*Mischung 5* in a 50.5μm cell at 30°C) we have marked the onset voltage of the first instability as a function of AC frequency. Below the critical voltage U_C, the sample is uniform. Above U_C we find oblique rolls (below 23Hz) and normal rolls (23..49 Hz) at onset in the conduction regime. With increasing voltage other structures (fluctuating rolls, grid patterns and dynamic scattering mode) are also observed, they are not considered here.

Time Resolved Textures

In the dielectric regime, normal dielectric rolls (DR) appear as the first instability. In spite of the oscillatory character of the director deflections, the microscopic observations usually provide a stationary picture of the

dielectric rolls. The cut-off frequency is often much higher than time resolution of the human eye or TV video cameras, and one is left with the time averaged image as shown in Fig. 3a. This image was taken with a

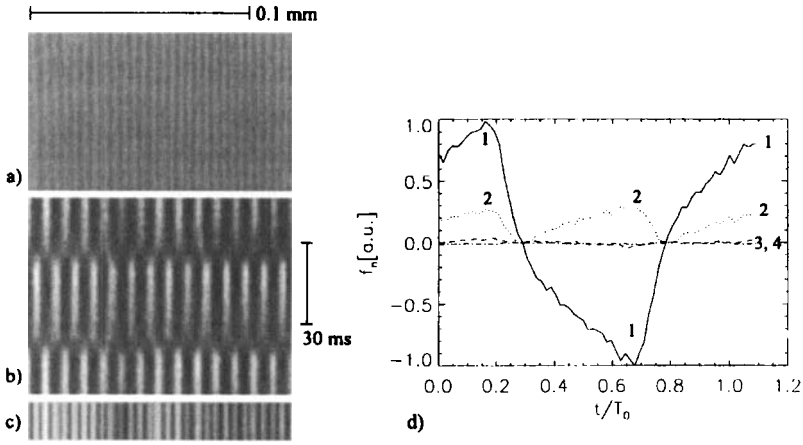

FIGURE 3 a) Experimental time averaged ('stationary') image of dielectric normal rolls (*Mischung 5* at f=16Hz, T=15.8°C, $U = 1.015U_C$). b) Time resolved image taken with a CCD line scan camera with exposure time 1ms (cross section normal to the rolls), same parameters as (a). c) Numerical time average of image (b), contrast enhanced. d) Time dependence of the amplitudes of the first four harmonics in the spatial Fourier expansions of image (b), the ground mode has a wavelength of 8.3μm and is equivalent to the spatial director modulation wavelength.

conventional CCD camera, setup 2a, and was averaged over 200ms (5 video images). However, the director field in the high frequency dielectric regime is rapidly oscillating with the excitation frequency, and the time averaged optical image provides only a part of the information about the director structure and dynamics. The oscillatory nature of the texture has been demonstrated already in early investigations of the scattering intensity of DR[3], and a time resolved measurement of the contrast amplitude of DR under high frequency sine excitation has been reported by Schneider et al.[14]. We have recorded time resolved images of cross sections normal to the convection rolls with the line scan camera and derive the relation

between director field and optical pattern. When the AC field is chosen close to the onset voltage of dielectric rolls, the wave vector of the rolls is uniform along x, the cross section taken normal to the convection rolls is sufficient to characterize the optical image. In order to increase the time resolution within the AC cycles the sample was cooled to 15.8°C where the cut-off decreases to 15Hz, and the sample was driven with f=16 Hz. Fig. 3b shows the spatio-temporal pattern, the time axis runs from bottom to top, slightly more than one cycle of the excitation frequency is shown. We have increased the signal to noise ratio in the image by adding 7 subsequent time periods of the AC frequency, i.e. we presuppose that the signal is periodic with T_0=1/f=62.5ms. This image does not change qualitatively when the voltage is changed in the existence range of the dielectric rolls, except for a change of the contrast amplitude. The spatial periodicity of the instant images has the doubled wavelength compared to the time averaged image. The image is not very sensitive with respect to the choice of the microscopic focus plane. The focus in the images presented in Fig. 3 has been chosen at the upper nematic/glass interface. We note that the contrast of the images has been enhanced in the reproductions with respect to the original image.

Figure 3c was obtained numerically by averaging each pixel row in image 3b. In the result, the wavelength of the 'stationary' texture is regained. The spatial period in the momentary images corresponds to the periodicity of the director field λ_0 while the time averaged stripe texture has half the period of the director tilt. The instant optical profiles along x have been Fourier transformed to gain quantitative information on the time dependence of the director field. The evolution of the Fourier coefficients of the first four harmonics is shown in Fig. 3d. The dominant ground mode (1) with period λ_0 changes its sign with the AC frequency and is completely absent in the 'stationary' time average while the second harmonics (2) retains its sign and determines the appearance of the stationary image. Higher harmonics are negligibly small. The relation between director tilt modulation and optical image can be established by optical simulations.

We have calculated the trajectories of light rays in the optically inhomogeneous medium on the basis of Fermat's principle[15]. Figure 4 shows the side view (xy plane) of a nematic layer with a momentary picture of the director tilt (dashed line) and the trajectories of normally incident light rays. (Note that the horizontal scale in Fig. 4 is stretched disproportionally.) The intensity profile at the upper plane of the nematic layer was

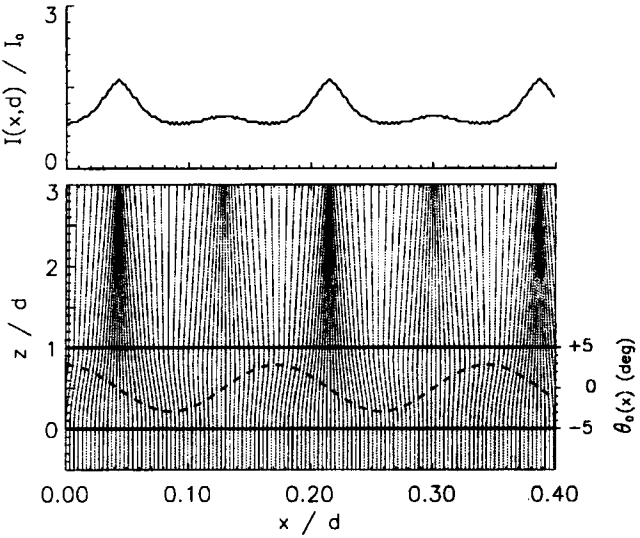

FIGURE 4 Side view of a nematic layer with trajectories of normally incident light. The director tilt is sketched by the dashed line (layer thickness d, lateral period of sine deformation 0.17d, ground mode $\theta_0 \sin(\pi z/d)$ along z, tilt amplitude 2.5°). The upper curve shows the intensity profile at the top of the nematic layer (z/d=1).

calculated from the density of 2000 transmitted light rays. The profile is shown in the top of Fig. 4. One has to remember that after half the period of the driving electric field the director deformation is inverted. In Fig. 4, this corresponds to a shift of the director pattern as well as the optical image by half the wavelength of the director modulation, $\lambda_0/2$.

We will now relate the time dependence of the texture with the director dynamics comparing simulated and measured textures. It is difficult to

extract absolute director deflections from the recorded images. Because of a certain offset in the line camera output (dark current of the CCD), we cannot compare absolute optical intensities. We will therefore restrict to a comparison of the intensity profiles, and we use the first and second harmonics of a spatial Fourier expansion of the optical images as shown in Fig. 3d.

In Figure 5, we show the simulated optical response which was obtained with model functions for the director tilt modulation

$$\mathbf{n} = (\cos\theta, 0, \sin\theta)$$

in the x, z-plane

$$\theta(x, z, t) = \vartheta(t)\sin(2\pi x/\lambda_0)\sin(\pi z/d)\,.$$

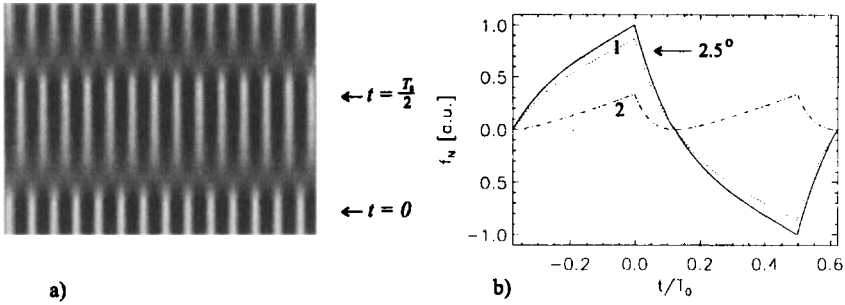

FIGURE 5 Calculated image (a) for 2.5° director tilt amplitude. An exponential time response of the director tilt as indicated by the dotted line of Fig. 5b was assumed (see text). The corresponding amplitudes of first (solid) and second (dash-dotted) harmonics are shown in (b).

The time dependence of the tilt amplitude $\vartheta(t)$ was approximated by a periodic sequence of exponential functions as proposed in the model by Smith et al.[3]. In Ref.[3], a system of two linearized coupled differential equations of charge and director fields was derived. The characteristic equation of this system yields periodic solutions

$$\vartheta = \vartheta_0\left[(1+e^{-a_1})e^{2a_2 t/T_0} - (e^{-a_1}+e^{a_2-a_1})e^{2a_1 t/T_0}\right] \quad (0 < t < T_0/2)$$

with $\vartheta(t + T_0/2) = -\vartheta(t)$, the parameters a_1 and a_2 are coupled by an additional condition[3] and depend upon frequency and strength of the electric field and wavevector λ_0 of the director pattern. In the simulation of Fig. 5, we have used a parameter set $a_1 = 0.8$ and $a_2 = -3.8$

For tilt amplitudes $\vartheta_{max} < 5°$, we obtain a satisfactory qualitative agreement between experimental and simulated images, as a comparison of Figs. 3 and 5 shows. In case of a sine driving voltage, most features of the spatio-temporal texture are the same but director response function and optical contrast are nearly sinusoidal in the time domain. The simulations do not allow to decide clearly whether in the director tilt deformation only the ground mode $\sin \pi z/d$ in z is present. Simulations of director fields with higher harmonics (e.g. $\theta(x, z, t) = \vartheta(t) \sin(2\pi x/\lambda_0) \tanh(10z/d) \tanh(1 - 10z/d)$) can produce comparable optical images, which are indistinguishable within experimental resolution.

In summary we can explain the observed spatio-temporal textures in the frame of standard theory with the assumption of an oscillating director field, a harmonic tilt modulation along x and a ground mode deformation normal to the cell plane. In addition to earlier experiments by Smith[3] and Schneider[14], the time resolved textures shown here provide a direct relation between the time dependent director field and optical image.

Chevron Formation

A well known phenomenon in the dielectric convection patterns which is not sufficiently understood so far is the formation of the chevron texture. When the voltage in the dielectric regime is increased by a few percent above the threshold value, the normal DR start to fluctuate, the spatial fluctuations of the wave vector are accompanied by the formation of defects. These defects move rapidly, mainly in the direction perpendicular to the rolls, and they are distributed chaotically in the sample plane. Only when the voltage is further increased above a certain threshold, the defects are aligned to chains and the so called chevron texture forms. This

evolution towards the chevron superstructure is depicted in Fig. 6 (upper image of each pair).

A theory describing a possible mechanism for chevron formation has been proposed recently by Rossberg et al.[21]. It predicts that the well known chevron texture in the dielectric regime involves a large scale periodical twist superstructure of the director field (a deflection out of the xz plane) in addition to the modulated tilt in the convection rolls.

In order to demonstrate the existence of this structure experimentally, we have modified the standard optical set-up. It has been shown previously[20] that the insertion of a phase plate as indicated in Fig. 2b between sample and analyzer allows the discrimination between oppositely twisted domains by different optical transmission intensities.

In Figure 6, a set of two images is compared at each reduced voltage. In both images, the analyzer is along $\vec{n}_0$ and a quarterwave plate is at 45° to $\vec{n}_0$. The top images (polarizer $\parallel \vec{n}_0$) are dominated by the stripe textures of the convection rolls which result from focussing of transmitted extraordinary light. The bottom images are taken with the polarizer perpendicular to the director, such that the convection rolls are no longer visible. In absence of a $\lambda/4$ plate, these textures are uniform. However, with the phase plate inserted, domains of right handed and left handed twist appear with different brightness. Near U_C where the defect-free normal rolls are found, the texture is uniform with a 'natural' brightness distribution (Fig. 6a). With the appearance of defects and beginning fluctuations of the rolls, local changes of the transmission intensity indicate the formation of an inhomogeneous twist structure (Figs. 6b,c) Below the threshold for the defect chain formation (Fig. 6c), the shape of the twist domains is elongated along x. Similarly, the defects in the roll structure are elongated (Fig. 6c) and propagate mainly perpendicular to the rolls. With the formation of the defect chains, the situation is reversed, as seen in Figs. 6d,e. The chevron superstructure of the convection rolls introduces a periodic stripe texture along y, and the twist domains correlate exactly with the topology of the chevrons.

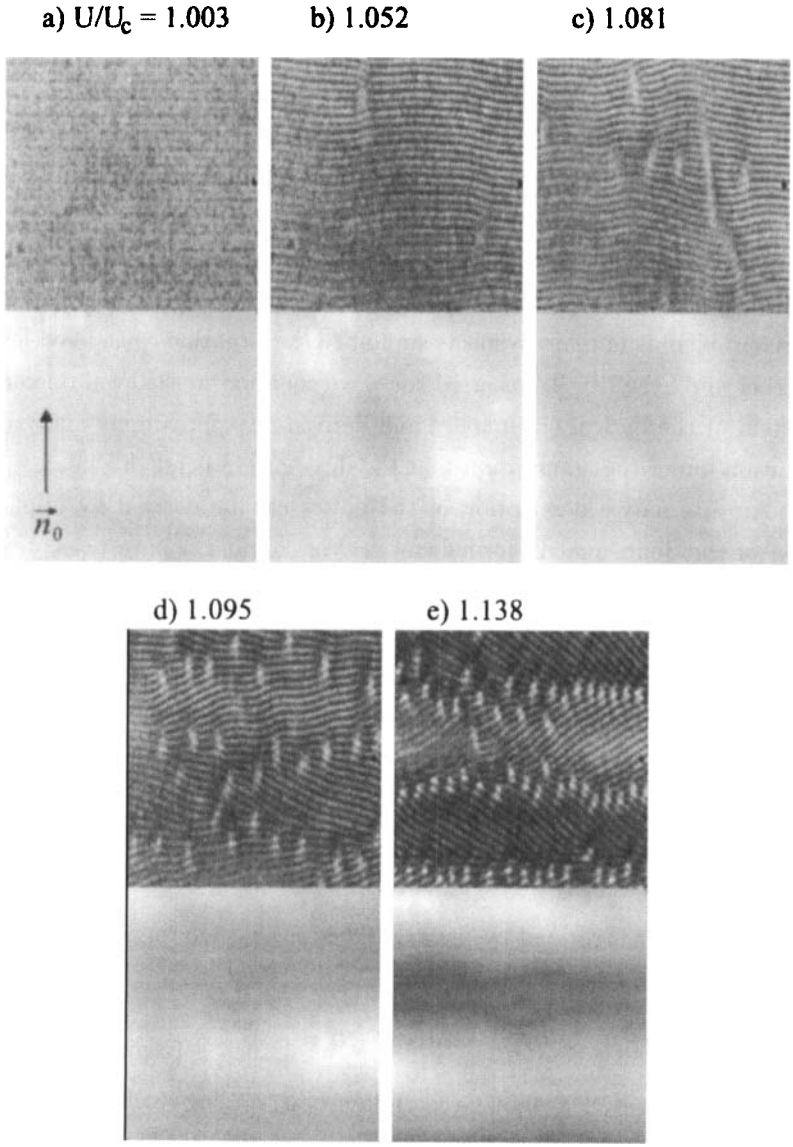

FIGURE 6 Transition from normal dielectric rolls at onset (a) via defect chaos to the chevron texture (e). The top image of each set is taken with the quarterwave plate inserted as in Fig. 2b and both polarizers along $\vec{n}_0$, while the bottom image shows the texture at the same reduced voltages with the polarizer rotated $\perp \vec{n}_0$. Image sizes are $125\mu m \times 125\mu m$.

Note that the second image in each set was taken about 2 seconds after the upper one. Relative positions of domains and defects in both images can therefore be shifted slightly due to the texture dynamics.

The optical contrast of the domains arises from the coupling of ordinary and extraordinary waves in the twisted director field. Wave coupling in planarly twisted director structures has been described earlier by Gerber and Schadt[16] who studied the magnetic twist Fréedericksz transition. This problem is in many respects similar to the situation considered here. Gerber and Schadt[16] transferred the wave equation to the local reference system of the optical eigenmodes and derived an approximate analytical solution under the assumption that the director gradients are small.

An alternative description of the optics can be derived by application of the Jones matrix formalism[17]. We consider a pure twist deformation $\vec{n} = (\cos\varphi(x,z), \sin\varphi(x,z), 0)$ of the director, with $\varphi(x,z) = \varphi_0(x)\sin(\pi z/d)$, and disregard for the first the director tilt modulation in the rolls. Since the lateral variations of φ_0 appear on a scale of several μm, we can locally assume plane waves. The Jones matrix for the propagation of normally incident light passing a nematic layer with thickness d_s and optical axis in the layer plane along x is

$$\overline{P}_0(d_s) = \begin{bmatrix} e^{i\kappa d_s} & 0 \\ 0 & e^{-i\kappa d_s} \end{bmatrix} \quad with \quad \kappa = \pi(n_e - n_o)/\lambda_{opt}$$

When the layer is rotated by the angle β about z, the propagation matrix has the form

$$\overline{S}(\beta)\overline{P}_0(d_s)\overline{S}(\beta)^{-1} \quad \text{with} \quad \overline{S}(\beta) = \begin{bmatrix} \cos\beta & -\sin\beta \\ \sin\beta & \cos\beta \end{bmatrix}.$$

The propagator for a thin layer of thickness Δz in which the director is uniformly twisted along z can be calculated analytically[19]. In a local coordinate system (X,Y,z) which rotates with the director it is found from the limit value

$$\overline{P}(\Delta z, \delta\varphi) = \lim_{m\to\infty} \left(\overline{P}_0(\frac{\Delta z}{m})\overline{S}^{-1}(\frac{\Delta\varphi}{m})\right)^m \tag{1}$$

where $\Delta\varphi$ is the total twist of the stack of m infinitesimally small layers.

In the approximation $1 \gg \kappa\Delta z \gg \Delta\varphi$ the propagator is

$$\overline{P}(\Delta z, \Delta\varphi) = \begin{bmatrix} 1 + i\kappa\Delta z & \Delta\varphi \\ -\Delta\varphi & 1 - i\kappa\Delta z \end{bmatrix}. \tag{2}$$

From this propagator we can derive a set of differential equations for the Jones polarization vectors

$$\frac{d\vec{E}}{dz} = \left(\lim_{\Delta z \to 0} \frac{\overline{P}(\Delta z, \Delta\varphi) - \overline{1}}{\Delta z} \right) \vec{E} = \begin{bmatrix} i\kappa & \varphi' \\ -\varphi' & -i\kappa \end{bmatrix} \vec{E} \tag{3}$$

$$\text{with} \quad \varphi' = \frac{d\varphi}{dz}.$$

In zero order approximation these differential equations yield the adiabatically guided waves $E_{X,Y}(z) = \exp\{\pm i\kappa z\}\, A_{e,o}$. Their amplitudes are not sensitive to a twist of the nematic. Wave coupling between these modes is mediated by the small off-diagonal elements $\pm\varphi'$, which lead to a weak amplitude modulation $A_{e,o}(z)$ of the zero order solutions introduced above.

For incident light polarized in y-direction, i. e. $A_e(0) = 0$, we can set $dA_o/dz \approx 0$ and arrive at

$$\frac{dA_e}{dz} = \varphi' \, \exp\{-2i\kappa z\} \cdot A_o. \tag{4}$$

This approximation holds for $\varphi' \lambda_{opt} \ll \pi(n_e - n_o)$, and we have confirmed the result by comparison with exact numerical calculations using Berreman's 4×4 matrix algorithm[18].

After integration with the z profile of the twist angle the complex amplitude

$$A_e(d) = i\,\varphi_0(x)\, f\, A_o(0) e^{-i\kappa d} \quad \text{with} \quad f = \frac{4\kappa\pi}{d} \frac{\cos(\kappa d)}{(\pi/d)^2 - (2\kappa)^2}. \tag{5}$$

is obtained. The normalized Jones vector at $z = d$ reads

$$\vec{E}(x) = \begin{pmatrix} i\,\varphi_0(x)\, f \\ (1 - \mathcal{O}(\varphi_0^2))\, e^{-i\kappa d} \end{pmatrix} \tag{6}$$

The incident linearly polarized light emerges from the cell with spatially varying ellipticity. An analyzer along $\vec{n}_0$ transfers this polarization grating into an intensity pattern $I(x)/I_0 = (\varphi_0(x)\, f)^2$ second order in the

small quantities f, φ_0. The resulting optical texture has half the wavelength of the corrsponding director structure but is usually too weak to be observed in the experiment. A more suitable detector can be constructed with a $\lambda/4$ phase plate in $\pm 45°$-position followed by the analyzer[20]. With the corresponding Jones matrices

$$\overline{P}_D = \frac{1}{\sqrt{2}} \begin{pmatrix} 1 & \pm i \\ 0 & 0 \end{pmatrix}$$

one obtains

$$\frac{I(x)}{I_0} \approx \frac{1}{2} \pm f \cos(\kappa d)\, \varphi_0(x) \tag{7}$$

The optical response is now first order in f and φ_0, opposite director twist causes opposite changes of the transmitted light intensity. The topology of the director twist structure is now directly visible. As already stated in Ref.[16], the slope of the optical response curve (Eq. 7) is very sensitive to the ratio d/λ_{opt}. In principle the optical characteristics could be optimized with monochromatic light, when wavelength and cell thickness are exactly adjusted to get integer $\kappa d/\pi$, but then the results depend crucially on the exact determination of the cell thickness. We have used white light and a B/W camera, and since for a 50.5μm cell the cosine term in Eq. 7 describes a rapidly oscillating function of λ_{opt}, a good estimate of the twist angle can be obtained from the averaged function

$$\frac{I(x)}{I_0} \approx \frac{1}{2} \pm \frac{2(n_e - n_o)d\bar{\lambda}_{opt}}{(\bar{\lambda}^2_{opt} - (2(n_e - n_o)d)^2}\, \varphi_0(x). \tag{8}$$

with an average optical wavelength $\bar{\lambda}_{opt} \approx 550nm$ and $\cos^2(\kappa d) \approx 1/2$. Using the substance parameters n_e=1.6315, n_o=1.4935 and the phase plate angle 45° we find

$$\frac{dI}{d\varphi_0} \approx -0.040 I_0 .$$

In the microscopic images of chevrons (Fig. 6) domains with twist $\varphi > 0$ and $\varphi < 0$ are equally present, and we can use the contrast of the textures (difference of transmission intensities I_+, I_- of oppositely twisted domains) as a quantitative linear measure for the twist amplitudes.

We conclude from an analysis of the images 6a-e that the fluctuation of the wave vector and formation of the chevron structure is accompanied by the appearance of director twist domains with twist angles comparable to the magnitude of the wavevector deflections. A detailed quantitative discussion will be given in Ref.[22].

SUMMARY

We have presented optical investigations of electroconvection patterns in nematic liquid crystals. We have shown that the time resolved images in the dielectric regime can be explained with standard assumptions for the nematic director field. A relation between director structure and optical texture was established. By application of optical simulations which are well known from the description of EHC structures in the conduction regime, we have obtained satisfactory agreement with the experimentally observed spatio-temporal pattern.

An investigation of the director field in the chevron structure was performed. By means of a phase plate inserted in the optical path we have visualized a twist superstructure in accordance with recent theoretical predictions[21]. At voltages below the formation of chevrons, fluctuations of the wave vector are accompanied by fluctuating director twist domains. After the emergence of the chevron texture with defect chains and a periodic modulation of the convection roll wave vectors, a strong correlation between chevrons and a periodic array of twisted domains is found. We have derived a quantitative relation between optical contrast and director twist amplitude using an analytical model for light propagation based on Jones propagation matrices.

Acknowledgments

This work was supported by the DFG with grant STA 425/3-1. We acknowledge A. Lindner who participated in optical experiments.

References

[1.] L. Kramer, and W. Pesch, Annu. Rev. Fluid Mech. **17** 515 (1995). L. Kramer, and W. Pesch, *Electrohydrodynamic Instabilities in Nematic Liquid Crystals* in "Pattern formation in Liq. Cryst." ed. A. Buka and L. Kramer, Springer, NY, and refs. therein.

[2.] E. F. Carr; J. Chem. Phys. **38** 1536 (1963), **39** 1979 (1963), **42** 738 (1969); Mol. Cryst. Liq. Cryst. **7** 253 (1969). W. Helfrich; *J. Chem. Phys.* **51** 4092 (1969).

[3.] I. W. Smith, Y. Galerne, S. T. Lagerwall, E. Dubois-Violette, G. Durand; *J. Physique Coll.* **C1** 237 (1975).

[4.] E. Dubois-Violette, P. G. de Gennes and O. Parodi; *J. Phys. (Paris)* **32** 305 (1971).

[5.] W. Zimmermann, and L. Kramer, *Phys. Rev. Lett.* **55** 402 (1985).

[6.] E. Bodenschatz, W. Zimmermann, and L. Kramer, *J. Phys. (Paris)* **49** 1875 (1988).

[7.] L. K. Vistin, A. Yu. Kabaenkov, S. S. Yakovenko; *Sov. Phys. - Crystallogr.* **26** 70 (1981).

[8.] K. Kondo, A. Fukuda, E. Kuze; *Jpn. J. Appl. Phys.* **20** 1779 (1981). K. Kondo, A. Fukuda, E. Kuze, M. Arakawa; *Jpn. J. Appl. Phys.* **22** 394 (1983).

[9.] H. Richter, S. Rasenat, I. Rehberg; *Mol. Cryst. Liq. Cryst.* **222** 219 (1992).
I. Rehberg, F. Horner, and G. Hartung; *J. Stat. Phys.* **64** 1017 (1991). S. Rasenat, G. Hartung, B. L. Winkler, I. Rehberg; *Exp. Fluids* **7** 412 (1989).

[10.] V. S. Mylnikov; *Opt. Spectrosc.***56** 177 (1984).

[11.] J. A. Kosmopoulos and H. M. Zenginoglou; *Appl. Optics* **26** 1714 (1987).

[12.] A. Joets and R. Ribotta; *J. Phys. (Paris)* **47** 595 (1986); *Opt. Commun.* **107** 200 (1994); *J. Physique I* **4** 1013 (1994).

[13.] H. Amm, *Diploma thesis* Leipzig 1997.

[14.] U. Schneider, M. de la Torre Juarez, W. Zimmermann, and I. Rehberg; *Phys. Rev. A* **46** 1009 (1992).

[15.] W. A. Newcomb, *Am. J. Phys.* **51** 338 (1983). S. Rasenat, G. Hartung, B. L. Winkler, I. Rehberg; *Exp. Fluids* **7** 412 (1989). A. Joets and R. Ribotta; *Opt. Commun.* **107** 200 (1994). S Rasenat, *Dissertation*, Bayreuth, Germany (1990).

[16.] P. R. Gerber, M. Schadt; *Z. Naturforsch.* **35A** 1036 (1980).

[17.] R. C. Jones; *J. Opt. Soc. Am.* **31** 488 (1941), **38** 671 (1948).

[18.] D. W. Berreman, and T. J. Scheffer, *Phys. Rev. Lett.* **25** 577 (1970). D. W. Berreman, *J. Opt. Soc. Am.* **62** , 502 (1972). S. Teitler, and B. W. Henvis, *J. Opt. Soc. Am.* **60** 830 (1970).

[19.] S. Chandrasekhar; Liquid Crystals, 2^{nd} edition, Cambridge University Press 1992. p. 213 ff.

[20.] M. Grigutsch, N. Klöpper, H. Schmiedel, and R. Stannarius. *Mol. Cryst. Liq. Cryst.*, **262** 283, (1995).

[21.] A. G. Rossberg, and L. Kramer, *Physica D* **115** 19 (1998).
[22.] In this approximation, we have assumed a planar pure twist deformation. The discussion of the influence of the director tilt and a quantitative comparison with numerical simulations is given elsewhere (H. Amm, R. Stannarius, and A. Roßberg, *Physica D* , submitted).